RSC Advances

ROYAL SOCIETY OF CHEMISTRY

www.rsc.org/advances

Graphical Abstract

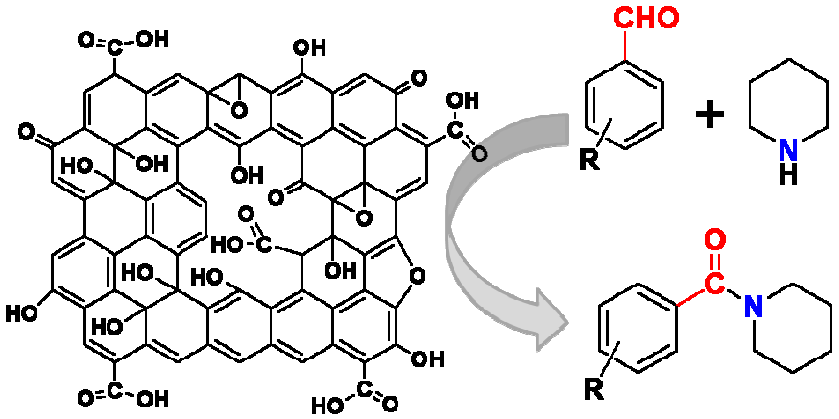

Graphene oxide was found to be a highly efficient carbocatalyst for one-pot synthesis of amides from aromatic aldehydes and secondary amine.

RSC Advances

RSC Publishing

ARTICLE

Metal-free one-pot synthesis of amides using graphene oxide as an efficient catalyst

Cite this: DOI: 10.1039/x0xx00000x

Shweta Kumari,[a] Amiya Shekhar,[a] Harshal P. Mungse,[b] Om P. Khatri,[b,*] and Devendra D. Pathak[a,*]

Received 10th July 2014
Accepted 00th xxxx

DOI: 10.1039/x0xx00000x

www.rsc.org/

Graphene oxide (GO) exhibiting high degree of oxygen functionalities and various structural defects was found to be a highly efficient and cost effective carbocatalyst for the one-pot base-free synthesis of amides from aromatic aldehydes and secondary amine. The chemical and structural features of GO as probed by FTIR, Raman, XRD and HRTEM analyses, were discussed to understand the catalytic mechanism for synthesis of amides. The present method obviates the use of transition metal catalysts and needs shorter reaction time.

Introduction

Amide is one of the most common functional groups present in the backbone of polymers, proteins, natural products, agrochemicals, pharmaceuticals, fragrances and dyes. Several methodologies have been addressed for synthesis of the amides by reaction of carboxylic acids, aldehydes, and alcohols with amines.[1-2] These reactions are catalysed by either salts or a bewildering range of complexes of transition metal such as manganese, iron, rhodium, ruthenium, iridium, zirconium, nickel, copper, silver, gold, palladium, and zinc.[3-4] Currently, oxidative amidation of aldehydes has becomes more attractive approach from economical and green chemistry point of view. In this context, various oxidants such as hydrogen peroxide, TBHP, oxone, NaOCl and molecular oxygen have been explored for amide synthesis.[5] However, most of these methods suffer from common drawbacks such as the use of precious transition metal catalysts which often involves multi-step and tedious synthesis, long reaction time, moderate yields, inert atmosphere and formation of by-products. Herein, our interest lies in exploring new route for metal- and base-free synthesis of amides from aromatic aldehydes and amines using a cost effective heterogeneous catalyst under mild reaction conditions.

Recently, graphene oxide (GO) has emerged as a versatile carbonaceous heterogeneous catalyst for a variety of organic transformations, such as oxidation of alcohols, thiols, sulfides, olefins etc; aza-Michael addition of amines to activated alkenes, acetalization of aldehydes, ring-opening polymerization of various cyclic lactones and lactams, Friedel-Crafts addition of indoles to α,β-unsaturated ketones, and oxidative coupling of amines to imines.[6-9] The renaissance of interest in the catalytic properties of GO has mainly arisen from its unique nanostructure, high specific surface area, presence of plenty of oxygen-containing functionalities and edge sites with unpaired electron.[10,11] Furthermore, low cost and scalable synthetic procedure of GO, promises its immense potential for various chemical transformation applications. Prompted by these reports, we, herein describe the synthesis of a series of amides from aromatic aldehydes and amine using GO as a readily available, inexpensive heterogeneous catalyst.

Experimental section

Preparation of GO

Initially, graphite oxide a precursor to GO was prepared by harsh oxidation of graphite powder using a mixture of $NaNO_3$, H_2SO_4 and $KMnO_4$ as strong oxidizing reagents. Then the oxidized product was treated with 30% solution of H_2O_2 in order to digest the unreacted content of $KMnO_4$. Subsequently, the product was rinsed and washed thoroughly with copious amounts of pure water to remove the excess content of soluble ions. The processed dark brown oxidized material known as graphite oxide was then exfoliated into the GO using an ultrasonic probe (VCX 500, Sonics & Materials, USA (tip diameter: 13 mm, intensity: 50%, time: 30 minutes)). Next, the exfoliated product was centrifuged at 5000 rpm for 15 minutes, which leads to two distinct phase, upper phase containing dispersible fine sheets of GO and lower deposited solid phase. The fine fraction (upper phase) of GO was dried at 80 °C and used for characterization and as a catalyst for amide synthesis.

Synthesis and Characterization of amides

The nicely dispersed 5 wt% GO in 5 mL water, prepared by sonication, was added to a reaction mixture of aldehyde (1 mmol) and piperidine (1 mmol) in acetonitrile (5 mL). The

reaction mixture was reflux for specific time (24 hr) under uninterrupted stirring. The progress of the reaction was monitored by TLC at regular intervals. After completion, the reaction mixture was cooled to room temperature and the GO catalyst was removed by filtration. The filtrate was treated with ethyl acetate (3 x 10 mL). The combined organic layers were treated with saturated brine solution and dried over anhydrous sodium sulphate. The removal of solvent yielded crude product which was purified by flash chromatography over silica gel G 60 and afforded the desired product. Furthermore, the synthesized amide products were analyzed by nuclear magnetic resonance (NMR) and Mass spectroscopies. The spectral data of synthesized amides are given below:

(4-Nitrophenyl)(piperidin-1-yl)methanone (3a) Yellow solid; ^{1}H NMR ($CDCl_3$) , 8.17 (d, 2H), 7.49 (d, 2H), 3.56 (br s, 2H), 3.04 (br s, 2H), 1.62 (br s, 4H), 1.49 (br s, 2H) ppm; MS (ESI) m/z 234 $[M+H]^+$.

(3-Nitrophenyl)(piperidin-1-yl)methanone (3b) Yellow solid; ^{1}H NMR ($CDCl_3$) , 8.24-8.29 (m, 2H), 7.69 (d, 1H), 7.62 (d, 1H), 3.80(br s, 2H), 3.41 (br s, 2H), 1.73 (br s, 4H), 1.52 (br s, 2H) ppm; MS (ESI) m/z 235 $[M+H]^+$.

4-(Piperidine-1-carbonyl)benzaldehyde (3c) Colorless oil; ^{1}H NMR ($CDCl_3$) , 10.0 (s, 1H),7.93 (d, 2H), 7.55 (d, 2H), 3.70 (br s, 2H), 3.29 (br s, 2H), 1.70 (br s, 4H), 1.52 (br s, 2H); MS ESI m/z 219 $[M+H]^+$.

3-(Piperidine-1-carbonyl)benzaldehyde (3d) Colorless oil; ^{1}H NMR ($CDCl_3$) , 9.99 (s, 1H), 7.98-7.93(m, 1H), 7.63 (d, 1H), 7.59 (t, 1H), 3.52 (br s,2H), 3.19 (br s, 2H), 1.62 (br s, 4H), 1.46 (br s, 2H) ppm; MS (ESI) m/z 220 $[M+H]^+$.

(4-Chlorophenyl)(piperidin-1-yl)methanone (3e) Colourless oil; ^{1}H NMR ($CDCl_3$) , 7.19 (d, 2H), 7.15 (d, 2H), 3.56 (br s, 2H), 3.14 (br s, 2H), 1.52 (br s,4H), 1.39 (br s, 2H) ppm; MS (ESI) m/z 224 $[M+H]^+$.

(2-Chlorophenyl)(piperidin-1-yl)methanone (3f) Yellow oil; ^{1}H NMR ($CDCl_3$) , 7.43-7.39 (m, 1H), 7.36-7.31 (m, 3H), 3.82-3.78 (m, 2H), 3.26-3.23 (m, 2H), 1.69-1.65 (m, 5H),1.43 (br s, 1H) ppm; MS (ESI) m/z 224 $[M+H]^+$.

(4-Bromophenyl)(piperidin-1-yl)methanone (3g) White solid; ^{1}H NMR ($CDCl_3$) , 7.72 (d, 2H), 7.50 (d, 2H), 3.51 (br s, 2H), 3.26 (br s, 2H); 1.49 (br s,4H), 1.33 (br s, 2H) ppm; MS (ESI) m/z 268 $[M+H]^+$.

Phenyl(piperidin-1-yl)methanone (3h) ^{1}H NMR ($CDCl_3$) , 7.25 (s, 5H), 3.42 (brs, 2 H), 3.39 (br s, 2H), 1.42 (br s, 4H), 1.35 (br s, 2H) ppm; MS (ESI) m/z 190 $[M+H]^+$.

(2-Hydroxyphenyl)(piperidin-1-yl)methanone (3i) Yellow solid; ^{1}H NMR ($CDCl_3$) , 9.70 (br s, 1H), 7.32-7.27 (m, 1H), 7.26 (d, 1H), 6.80 (d, 1H), 6.76 (t, 1H), 3.59 (t, 4H), 1.77-1.69 (m, 6H); MS (ESI) m/z 206 $[M+H]^+$.

Chemical and Structural Characterization of GO

The fourier infrared (FTIR) spectrum of GO was carried out by using a Thermo-Nicolet 8700 Research spectrophotometer with a resolution of 4 cm^{-1}. Raman spectrum of GO was collected using a Renishaw micro-spectrometer at an excitation wavelength of 514.5 nm. The powder-X-ray diffraction (XRD) analyses of GO was carried out using a Bruker D8 Advance diffractometer at 40 kV and 40 mA with Cu-Kα radiation (λ = 0.15418 nm). The BET surface area and pore size distribution of GO was calculated by their N_2 adsorption/desorption isotherms using a BelsorbMax, BEL, Japan. The high resolution microscopic features of GO nanosheets was examined on the high resolution transmission electron microscope (HRTEM) by drop casting of their ethanolic solution on the TEM grid.

Results and discussion

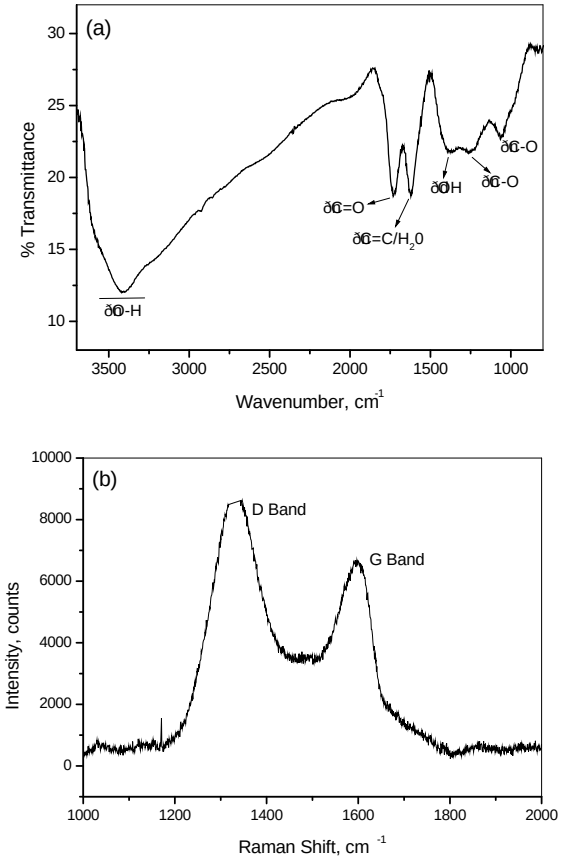

Figure 1 Chemical characterization. (a) FTIR and (b) Raman spectra demonstrating the chemical functionalities and defects

The GO was prepared by the harsh oxidation of graphite powder and then exfoliation of oxidized product by sonication. The chemical and structural features of GO were elucidated by FTIR, Raman, XRD and HRTEM analyses. The FTIR spectrum of GO (Fig. 1a) exhibited strong characteristics bands at 3419 cm^{-1} (O-H stretch attributed to alcohol and phenol groups), 1732 cm^{-1} (C=O stretch ascribed to carboxyl and carbonyl groups), 1622 cm^{-1} (an overlapped signature of bending modes of trapped water molecules and un-oxidized sp^2 carbon domain), 1372 cm^{-1} (O-H bending), 1263 cm^{-1} (C-O stretch attributed to phenols, epoxy and ether groups), and 1065 cm^{-1} (C-O stretch associated to hydroxyl groups). These vibrations revealed the presence of hydroxyl, epoxy, carboxyl, carbonyl, phenolic etc. functional groups in the GO scaffold. The [12]

oxygen functionalities located in the basal plan of GO scaffold, disturb the sp^2 electron conjugated network and generates various sp^3 defects and sp^3 carbon centres, as deduced by micro-Raman analysis. The Raman spectrum of GO (Figure 1b) exhibited two characteristics bands at 1597 and 1354 cm^{-1} correspond to G (graphitic band) and D (defects band) modes, respectively. The shift in the G band towards higher wave number is attributed to overlap of the G band with the D band due to presence of various strucral defects, discrete sp^2 domains separated by oxygen-containing functional groups and limited number of layers in the GO.[13]

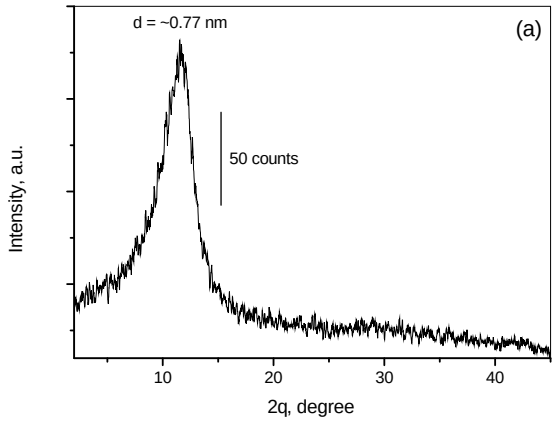

Figure 2. Structural characterization (a) XRD and (b) Raman analysis of GO.

The XRD pattern of GO (Figure 2a) shows a broad diffraction peak at $2\theta = 11.48°$ with a corresponding d spacing of 0.77 nm, which is very large compared to the graphite. The ample oxygen functionalities in the basal plane of GO along with absorbed water molecules increased the interlayer distance. Furthermore, nanoscopic features of GO were probed by HRTEM analysis. Figure 2b shows the wrinkled and crumpled features in HRTEM image of GO nanosheets. These sheets are aggregated in a considerably disordered manner. The sp^3 carbon centres associated to the oxygen functionalities and various structural defects in the basal plane of GO disturbed the two dimensional structure, resulting in roughened surface with lot of folded and crumpled features. The high resolution image of GO illustrate very small size of disordered domains, which are highlighted by the red arrows. These sites could be associated to the defect sites and holes. Recently, aberration corrected HRTEM images of GO have shown highly inhomogeneous structure, having three major regions: holes, graphitic domains (sp^2 domain) and disordered regions (blend of sp^3 and sp^2 carbons, indicating areas of high oxidation) with approximate area of 2%, 16% and 82%, respectively.[14] Scanning tunnelling microscope imaging have also revealed the porous nature of reduced GO. The edge sites in the holes and periphery of sheets with unpaired electrons constitute the active catalytic sites, which enhanced the trapping and activation of molecular oxygen for the oxidative coupling of amines to imines.[9] The high BET surface area (103. 7 $m^2.g^{-1}$) of GO as extracted from the nitrogen adsorption / desorption isotherm (Figure 3), promises the potential of GO for heterogeneous catalytic activities. Besides that, presence of ample oxygen functionalities in the GO provide its stable and homogeneous dispersion in the aqueous media (water), which function as pseudo-heterogeneous catalyst for efficient chemical transformation with the added benefits of facile recovery of the GO catalyst.

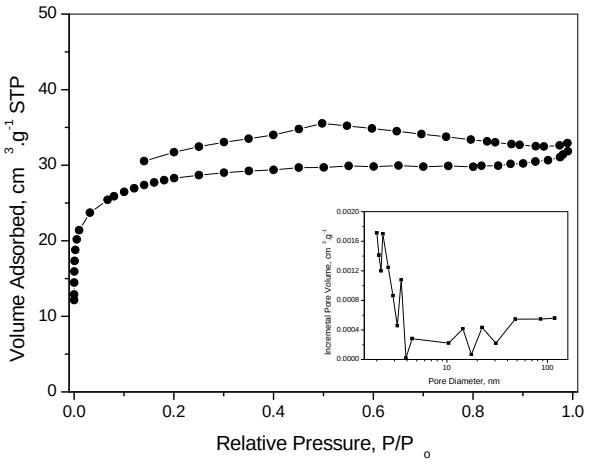

Figure 3. N_2 adsorption/desorption isotherms and pore size domains are highlighted by red.

The catalytic potential of GO was explored for the synthesis of amides from aromatic aldehydes and piperidine, as shown in Scheme 1.

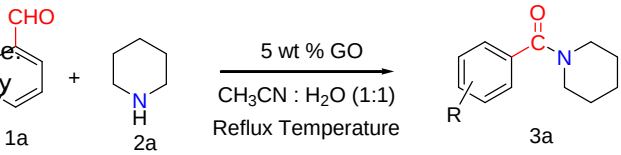

Scheme 1. GO catalyzed synthesis of amides from aromatic aldehydes and amine.

Table 1. Reaction between 4-nitrobenzaldehyde (1 mmol) and piperidine (1 mmol) under different reaction conditions

Entry	Catalyst	Temperature, °C	Time, h	Yield, %[a]
1	-	rt	72	Nil
2	-	140	24	Nil
3	5 wt% of GO in water	rt	36	55
4	5 wt% of GO in water	100	08	82

[a] Isolated yield after work up

Initially, the reaction of piperidine (1 mmol) with 4-nitrobenzaldehyde (1 mmol) in 5 ml acetonitrile was chosen as a model reaction to optimize the reaction conditions. When the reaction was carried out without catalyst (Table 1, entry 1) at room temperature, no product was obtained even after 3 days. The reaction at high temperature (140 °C) in absence of catalyst also did not yield any product (Table 1, entry 2). The reaction in presence of 5 wt % of GO in water (5 ml) at room temperature afforded 55% yield in 36 h (Table 1, entry 3). However, to our delight, the same reaction under identical conditions but at reflux temperature (100 °C) yielded 82% of desired product within 8 hr (Table 1, entry 4).

Table 2. Solvent effects on the reaction of 4-nitrobenzaldehyde (1 mmol) and piperidine (1 mmol) under reflux condition using 5 wt% GO dispersion as a catalyst

Entry	Solvent	Time, h	Yield, %[a]
1	Water	11	40
2	Methanol	18	15
3	Ethanol	15	20
4	Toluene	14	35
5	Acetonitrile	10	60
6	Ethyl acetate	12	trace
7	Acetonitrile : Water (1:1)	08	82
8	Acetonitrile : Water (1:2)	08	50
9	Acetonitrile : Water (2:1)	08	65

[a] Isolated yield

Furthermore, in order to explore the effect of solvents, the reaction was carried out in different solvents. The water as reaction media could afford 40 % yield of desired product (Table 2, entry 1). The reaction in methanol, ethanol, toluene, and acetonitrile gave yields; 15, 20, 35, and 60 %, respectively (Table 2, entries 2-5). Ethyl acetate was found to be the worst solvent (Table 2, entry 6) as no product could be isolated. The mixtures of acetonitrile and water in different ratio (v/v) of 1:1, 1:2, and 2:1 gave 82, 50, and 65% yields of product, respectively (Table 2, entries 7-9). Gratifyingly, the optimum yield (82%) of the product was obtained when the reaction was carried out in a 1:1 mixture of acetonitrile and water under reflux condition for the 8 h. The scope of the reaction was further extended to different aromatic aldehydes bearing various functional groups on ortho-, meta- and para- positions, with piperidine under the optimized conditions and the results obtained, are summarized in Table 3. The products were obtained as colourless oil to brick-red crystalline solids, soluble in common organic solvents such as chloroform, methanol, ethanol, DMSO and were fully characterized by ^{1}H NMR and Mass spectra. The electronic effect introduced by substitution of the aromatic aldehyde had insignificant influence on the yields of corresponding amide. The reaction could tolerate both electron-withdrawing groups (Table 3, entries 1-7) and electron-donating groups (Table 3, entries 8-9) with good yields (60 - 82%). It was noted that benzaldehyde bearing a strong electron-withdrawing group like nitro afforded the corresponding product with an excellent yield (Table 3, entries 1-7). However, steric bulk functional groups had a negative influence on this reaction, particularly on ortho- and meta-positions. For instance, meta-substituted -CHO groups disfavored the reaction progress and solidized the product yield (Table 3, entries 3,4). However, presence of small functional groups on ortho-position had no significant effect on their corresponding product yields (Table 3, entries 5,6). These results revealed that the product yields were dependent on the substituent's position on the benzaldehyde ring. The reaction of primary amines (aniline, 2-chlorobenzenamine and 2-aminophenol) in place of secondary amines, with same aldehydes did not succeed to yield the expected amide products, thereby limiting the scope of the reaction. Recently, Wong et al. have reported $KAuCl_4$-catalysed synthesis of amides from the aromatic aldehydes and piperidine (1:2 equivalent molar ratio),[4d] however, the converted yields were quite low compared to the GO-catalyzed system, where aromatic aldehydes and piperidine were used in 1:1 equivalent molar ratio. The observed high yield of amides is associated to the unique nanostructural and chemical features of GO.

Table 3. Synthesis of amides from various aldehydes and piperidine in presence of GO catalyst under the optimized reaction conditions

Entry	Aldehydes	Product[a]	Time, h	Yield, %[b]
1	 1a	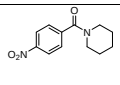 3a	8.0	82
2	 1b	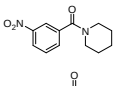 3b	11.5	70
3	 1c	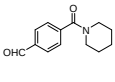 3c	9.5	77
4	 1d	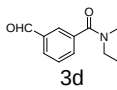 3d	13.5	60
5	 1e	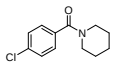 3e	13.5	79
6	 1f	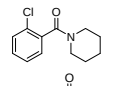 3f	10.0	79
7	 1g	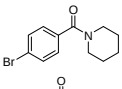 3g	12.5	65
8	 1h	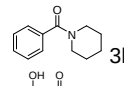 3h	14.0	68
9	 1i	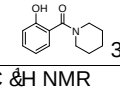 3i	13.0	75

[a] Purity determined by TLC & ^{1}H NMR
[b] Isolated yield after work up

The mechanistic aspect of the reaction is ambiguous at present although a free radical mechanism involving an aminyl radical has been propounded in case of Au(III)[4d] and an imine intermediate for Ru(II), Rh(III)- or Ir(III)-, catalysed synthesis

of amides.[15] We speculate that the unpaired electrons present at the edge of GO[16,9] react with the atmospheric oxygen to generate $O_2^{\bullet-}$, which subsequently reacts with secondary amine to generate aminyl radical, (I_1). The reaction of aminyl radical with an aldehyde may generate an alkoxy radical (I_2), which after β-radical elimination, yields the desired amide product (Scheme 2). The presence of bulkier group in ortho- and meta-position of benzaldehyde further, hindered the formation alkoxy radical (I_2) owing to steric hindrance, as a result, benzaldehyde with bulkier ortho- and meta-substitution provided lower yields (Table 3, entries 3,4). The evidence for participation of atmospheric oxygen as oxidant comes from the fact that when the reaction was carried out under an inert atmosphere (nitrogen), no product formation was observed. Recently, Loh et al. carried out electron spin resonance studies of reduced GO and revealed the presence of bonding π-electron at the edge of reduced GO, which are analogous to non-kekule molecules having open shell unpaired electrons and function as active catalytic sites for activation of molecular oxygen by a sequence of electron transport and reduction to superoxide radical.[14b] Furthermore, it has been noted that high polar nature of GO show excellent affinity towards the polar reactants aldehydes and secondary amines, where theses precursors could easily available to proceed the reaction by catalytic role of GO.

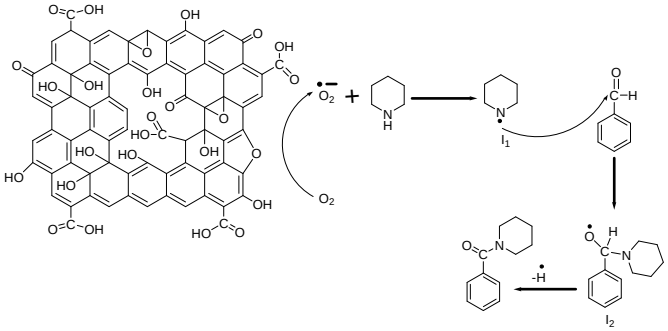

Scheme 2 Proposed reaction mechanism for the formation of amides

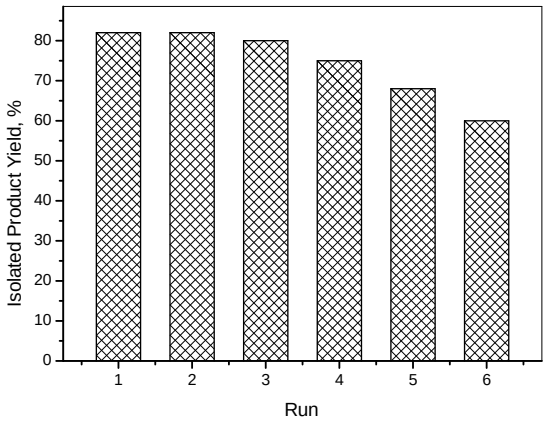

Figure 4 Recycle of GO catalyst for the reaction between 4-nitrobenzaldehyde and piperidine

The recyclability of GO catalyst was evaluated by choosing a reaction between 4-nitobenaldehyde and piperidine as a model reaction. After completion of reaction, the catalyst could easily be separated out by filtration from the aqueous layer, then washed with dichloromethane for the subsequent batch of reaction. It is apparent from Figure 4 that the GO catalyst could be reused up to two cycles without loss of catalytic activity. However, third cycles onwards, gradual decline in the catalytic activity of GO was noted. These results revealed that the chemical and structural features, which are responsible for catalytic activity of GO, were gradually changed with increasing the number of reaction cycle. Recently, it has been established that GO undergoes partial deoxygenation at moderate temperature (100 °C), consequently, the chemical and structural features of GO changed as a function of hydrothermal time.[17] Herein, amide preparation reactions were carried out at 100 °C, which might have changed the chemical and structural features of GO, as a result, gradual decline of catalytic activity. Despite these facts, considering the low cost, ease of preparation and free from metals, GO promises its potential not only for industrial applications but also addressed the environment benign synthetic methodology for the various amides.

Conclusions

In summary, the GO has been found to be an efficient, economic and heterogeneous carbocatalyst for the synthesis of amides from a variety of aromatic aldehydes and piperidine. These reaction afforded good-to-excellent product yields and the GO catalyst could be easily recovered. To the best of our knowledge, this is the first report on GO catalyzed one pot synthesis of amides.

Acknowledgements

We are thankful to the SAD and RTD of IIP for providing help in the analysis of the samples. SK and HM acknowledges the receipt of ISM and UGC fellowship.

Notes and references

[a] Department of Applied Chemistry, Indian School of Mines, Dhanbad 826004, India.
[b] Chemical Science Division, CSIR Indian Institute of Petroleum, Dehradun- 248005, India
*Email: ddpathak@yahoo.com (DD Pathak), opkhatri@iip.res.in (OP Khatri)
Phone number: +91 9431126250.

1 (a) C. A. G. N. Mobtalbetti and V. Falque, Tetrahedron, 2005, 61, 10827-10852; (b) V. R. Pattabiraman and J. W. Bode, Nature, 2011, 480, 471-479.
2 (a) C. Gunanathan, Y. Ben-David and D. Milstein, Science, 2007, 317, 790-792; (b) L. U. Nordstrom, H. Vogt and R. Madsen, J. Am. Chem. Soc. 2008, 130, 17672-17673; (c) R. Cadoni, A. Porcheddu, G. Giacomelli and L. D. Luca, J. Org. Lett. 2012, 14, 5014-5017.
3 (a) R. Vanjari, T. Guntreddi and K. N. Singh, Org. Lett., 2013, 15, 4908-4911; (b) B. Anxionnat, A. Guérinot, S. Reymond and J. Cossy, Tetrahedron Lett. 2009, 50, 3470-3473; (c) H. Peng, L. Xu, H. Wu,

K. Zhang and P. Wu, Chem. Commun., 2013, 49, 2709-2711; (d) B. Kang, Z. Fu and S. H. Hong, J. Am. Chem. Soc., 2013, 135, 11704-11707; (e) N. A. Owston, A. J. Parker and J. M. J. Williams, Org. Lett., 2007, 9, 73-75; (f) B. N. Atkinson, A. R. Chhatwal, H. V. Lomax, J. W. Walton and J. M. J. Williams, Chem. Commun., 2012, 48, 11626-11628.

4 (a) L. Field, P. Barnett, S. H. Shumaker and W. S. Marshall, J. Am. Chem. Soc., 1961, 83, 1983-1987; (b) S. K. Sharma, S. D. Bishopp, C. L. Allen, R. Lawrence, M. J. Bamford, A. A. Lapkin, P. Plucinski, R. J. Watson and J. M. J. Williams, Tetrahedron Lett., 2011, 52, 4252-4255; (c) R. S. Ramón, J. Bosson, D. Díez-González, N. Marion and S. P. Nolan, J. Org. Chem., 2010, 75, 1197-1202; (d) G. L. Li, K. K. Y. Kung and M. K. Wong, Chem. Commun., 2012, 48, 4112-4114; (e) C. L. Allen, C. Burel and J. M. J. Williams, Tetrahedron Lett., 2010, 51, 2724-2726.

5 (a) X. Liu and K. F. Jensen, Green Chem., 2013, 15, 1538-1541; (b) K. R. Reddy, C. U. Maheswari, M. Venkateshwar and M. L. Kantam, Eur. J. Org. Chem., 2008, 3619-3622; (c) J. Gao and G. W. Wang, J. Org. Chem., 2008, 73, 2955-2958; (d) J. Liang, J. Lv and Z. Shang, Tetrahedron, 2011, 67, 8532-8535; (e) J. F. Soule, H. Miyamura and S. Kobayashi, J. Am. Chem. Soc., 2011, 133, 18550-18553; (g) E. Sindhuja, R. Ramesh, S. Balaji, and Y. Liu, Organometallics, 2014, dx.doi.org/10.1021/om500556b.

6 (a) D. R. Dreyer, H-P. Jia and C. W. Bielawski, Angew. Chem. Int. Ed., 2010, 49, 6813-6816; (b) H. P. Jia, D. R. Dreyer and C. W. Bielawski, Adv. Synth. Catal., 2011, 353, 528-532; (c) D. R. Dreyer, H. P. Jia, A. D. Todd, J. Geng and C. W. Bielawski, Org. Biomol. Chem., 2011, 9, 7292-7295; (d) D. R. Dreyer and C. W. Bielawski, Chem. Sci., 2011, 2, 1233-1240.

7 (a) S. Verma, H. P. Mungse, N. Kumar, S. Choudhary, S. L. Jain, B. Sain and O. P. Khatri, Chem. Commun., 2011, 47, 12673-12675; (b) A. Dhakshinamoorthy, M. Alvaro, M. Puche, V. Fornes, and H. Garcia, Chem. Cat. Chem., 2012, 4, 2026-2030.

8 (a) A. V. Kumar and K. R. Rao, Tetrahedron Lett., 2011, 52, 5188-5191; (b) D. R. Dreyer, K. A. Jarvis, J. P. Ferreira and C. W. Bielawski, Polym. Chem., 2012, 3, 757-766.

9 C. Su, M. Acik, K. Takai, J. Lu, S. Hao, Y. Zheng, P. Wu, Q. Bao, T. Enoki, Y. J. Chabal and K. P. Loh, Nature Commun., 2012, 3, 1298.

10 C. Su and K. P. Loh, Acc. Chem. Res., 2013, 46, 2275-2285.

11 S. Navalon, A. Dhakshinamoorthy, M. Alvaro and H. Garcia, Chem. Rev., 2014, 114, 6179-6212.

12 (a) T. Szabo, O. Berkesi and I. Dekany, Carbon, 2005, 43, 3186-3189; (b) A. Bagri, C. Mattevi, M. Acik, Y. J. Chabal, M. Chhowalla and V. B. Shenoy, Nat. Chem., 2010, 2, 581-587; (c) H. P. Mungse, O. P. Sharma, H. Sugimura and O. P. Khatri, RSC Adv., 2014, 4, 22589-22595.

13 (a) K. N. Kudin, B. Ozbas, H. C. Schniepp, R. K. Prud„homme, I. A. Aksay and R. Car, Nano Lett., 2008, 8, 36; (b) G. K. Ramesha and S. Sampath, J. Phys. Chem. Lett., 2009, 113, 7985.

14 (a) K. Erickson, R. Erni, Z. Lee, N. Alem, W. Gannett and A. Zettl, Adv. Mater., 2010, 22, 4467-4472; (b) K. P. Loh, Q. Bao, G. Eda, M. Chhowalla, Nature Chem., 2010, 2, 1015-1024.

15 N. Raja and B. Therrien, J. Organomet. Chem., 2014, 765, 1-7.

16 (a) M. Wang, X. Song and N. Ma, Catal. Lett., 2014, 144, 1233-1239; (b) L. S. Bai, X. M. Gao, X. Zang, F. F. Sun and N. Ma, Tetrahedron Lett., 2014, dx.doi.org/10.1016/j.tetlet.2014.06.097.

17 S. Choudhary, H. P. Mungse and O. P. Khatri, Chem. Asian J., 2013, 8, 2070-2078.